International Conference on Applied Energy 2019
Aug 12-15, 2019, Västerås, Sweden
Paper ID: 961

COMPARATIVE STUDY ON INDOOR COMFORT OF COLD TIBETAN AREAS WITH ACTIVE AND PASSIVE SOLAR HEATING SYSTEM

Bo Zhang [1,2,3,4], Zhaofu Wang [1,2,3,4], Jinping Li [1,2,3,4]*, Juanjuan Huang [1,2,3,4]

Chunlong Wang [1,2,3,4]

(1. Lanzhou University of Technology, Western China Energy & Environment Research Center, Lanzhou 730050, China;
2. China Northwestern Collaborative Innovation Center of Low-carbon Urbanization Technologies, Lanzhou 730050, China;
3. Key Laboratory of Complementary Energy System of Biomass and Solar Energy, Gansu Province, Lanzhou 730050, China;
4. Lanzhou University of Technology, College of Energy and Power Engineering, Gansu Province, Lanzhou 730050, China)

ABSTRACT

Winter heating, as a basic need of the public, takes great effects on living habits and living level. In Gannan Tibetan Autonomous Prefecture, winter is cold and winter heating lasts for 7 months. Passive solar building technology has been advocated and spread for energy-saving and living standard improving since 1970s. At present, coal and dry cow manure are usually burned in stove for heating and indoor comfort is still unknown for the passive solar building. Considering clean heating with solar energy, an active solar heating system was developed in a passive solar building with low temperature floor irradiator and water heating Kang and indoor comfort of a passive solar building with active solar heating was compared to that with stove heating by on-site experiments and PMV-PPD method. The experimental results show that, in a whole heating season, the indoor temperature of five sevenths days meet the Standard of GB50785-2012 and humidity always meets the Standard and the concentrations of CO, SO_2, NO_2, PM10, PM2.5 and CO_2 are always below the Standard Values in GBT18883-2002 in the passive solar building with active solar heating, while in the passive solar building with stove heating, the indoor temperature usually does not meet the Standard and the concentrations of CO, SO_2, NO_2, CO_2, PM2.5 and PM10 are always higher than that of the passive solar building with active solar heating and the concentrations of PM2.5 and PM10 are always higher than the Standard Values in GBT18883-2002. According to the evaluation of PMV-PPD index and IAQ index, active solar heating show more favorable performances than stove heating in a passive solar building. Hence, in cold Tibetan areas, it is promising for active solar heating to take the place of stove heating in aspects of energy-saving and indoor air quality improving.

Keywords: solar active and passive heating system, indoor thermal environment, indoor air quality, indoor comfort

1. INTRODUCTION

Gannan Tibetan Autonomous Prefecture, situated in the southwest of Gansu Province, is one of the ten Tibetan Autonomous Prefectures in China. It is located in the transition zone between the Qinghai-Tibet Plateau and the Loess Plateau. In this area, the annual mean temperature is low and the temperature varies greatly between day and night, however, the solar radiation resources is abundant. Therefore, it is of great significance that using the solar energy meet the local building’s energy consumption.

Solar heating technology is divided into the active and the passive. At present, domestic and foreign scholars have conducted many researches on solar heating. Trombe wall is one of the passive solar systems. Stazi F et al[1] developed an experimental study on the behavior of Trombe walls in a residential building under a Mediterranean climate and carried dynamic simulations with software EnergyPlus. The conclusion demonstrated that Trombe wall could save heating energy and upgrade the thermal comfort in winter and intermediate seasons. In summer solar walls determine an increase in cooling energy needs and risk of overheating. Jie J et al[2,3] designed a new PV-Trombe wall(PVTW) and carried out experimental research. The indoor temperature with PV-Trombe wall kept 13.4℃ among 7 days and the PV efficiency was increased by 5%. Rabani M et al[4] designed a new Trombe wall which absorbed solar radiation from three directions (East, South and West) and carried out experimental research. The results revealed that the indoor temperature on the coldest days in Yazd city (Iran) was kept within 15–30 ℃, Sunspace is another the passive solar system. Sánchez-Ostiz et al[5] tested sunspaces under real conditions in Spain and nine scenarios during winter 2011 and summer 2012. The Results showed that sunspaces with heat storage could take well advantage of the solar energy and the adjacent room had a better indoor thermal performance in winter and summer. Oliveti G et al[6] estimated the solar radiation energy absorbed by the sunspace and the thermal comfort was estimated by the operative temperature. Y. Yang[7] carried out an on-site study on the single buildings with sunspace in China. The results show that the sunspace can improve the indoor thermal comfort but have a negative effect on indoor lighting and ventilation. At present, solar heating system is generally made up of different components. D. Zhao et al[8] designed a system consisting of solar Kang and solar air heating systems. The solar air heating system satisfies the daytime heating demand, and the solar Kang stores energy during the daytime and provides a good sleeping environment at night. M. Nemś et al[9] introduced the experiment which is made of centralized solar collectors and rock layers, and verified the correctness of the mathematical model. A. Carotenuto et al[10]studied a heating and cooling system with renewable energy, which used dynamic simulation models and energy economic analysis methods. Issam Sobhy et al[11] conducted numerical and experimental studies on the energy characteristics and economics of traditional bathhouses with solar floor heating systems, and found that solar heating systems with heat storage have significant benefits on energy-saving and environment-protection. Ali et al[12] analyzed the real-time performance of a small-capacity tower solar hot water heating system in Taksi, Pakistan, and verified the simulation results through experiments. Shan M et al[13] built an integrated space heating system including passive sunspace, active solar water heating, and air-source heat pump (ASHP), and comparatively analyzed in a full-scale test house in a cold climate zone. This integrated system showed many encouraging results in terms of the maintenance of a stable and comfortable indoor thermal environment during the winter season. Badescu V et al[14] studied an active solar heating system which provided domestic hot water and winter heating. The results show that this pattern is not suitable for solar heating system.

To sum up, solar heating could really greatly improve indoor thermal comfort, domestic and foreign scholars have not yet combined active solar floor heating technology, water heating Kang technology and passive sunspace together for winter heating. This study is of great significance to improve the backward heating method in Tibetan area.

2. MATERIAL AND METHODS

2.1 Experimental object

The experimental objects are two similar single buildings with additional sun-space, located in the Shanglangkanmu Village in Gannan Tibetan Autonomous Prefecture, Northwest China. The external view of building is shown in Fig. 1.

Fig. 1 External view of the building

The building area is 170m^2. The exterior wall of the building consists of three parts. The exterior is made of stone and pile, about 650 mm, the interior is a wooden board with a thickness of 50 mm and there is an air layer of about 100 mm between the two. The interior of the house is separated by 50 mm boards. One of them used cow dung stove to heat and is regarded as a comparative building and the other is regarded as an experimental building. The experimental building adopts the solar active heating system heating, and the heating system diagram is shown in Fig. 2.

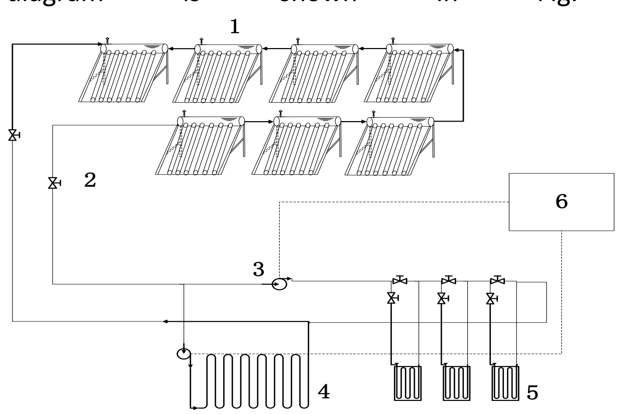

Fig.2 Solar active heating system diagram
1. Vacuum tube solar collector array 2. Ball valve 3. Heating circulating pump
4. Radiant floor 5. Radiant bed 6. Control cabinet

The system includes the solar heat collector array, the heating circulation pump, radiant floor, radiant bed, the control cabinet and ball valve. The solar collector array includes 7 sets of solar vacuum tube collector produced by the Sun Bridge Company. The length of vacuum tube is 1.8 m, the diameter of the tube is 58 mm, and the volume of the heat collector tank is 250 L. The floor heating coil pipe adopts PE-RT pipe, and its diameter is 20 mm. The coil pipe is arranged in a roundabout way, and the pipe spacing is about 200 mm. Solar active heating system adopts time control strategy, there are two modes of daytime anti-freezing and night heating. The anti-freezing mode operation time is 8:00~18:00, each hour heating pump runs 5 min, such as: 8:00~8:05 pump operation, 8:05~9:00 pump stop operation; the heating mode operation time is 18:00~8:00, each hour pump runs 30 min, such as 18:00~18:30 pump operation, 18:30~19:00 pump stops running.

2.2 Methods

Referring to the “Civil Building Indoor Thermal and Humidity Environmental Evaluation Standard” (GB/T 50785-2012)[15], the test point layout of the experimental building is shown in Figure 3. The measuring points A~M are arranged with temperature measuring points, where A and C are ground temperature measuring points, which are arranged at two equal points of the ground diagonal respectively. Four points about indoor air temperature are measured on B, at vertical heights of 0.1 m, 0.6 m, 1.1 m and 1.7 m respectively. At the same time, indoor wind speed and indoor humidity measuring point are also arranged at 1.7 m. Points D~J are wall temperature measuring points, 1.5 m from the ground and point K is inter-sunlight air temperature measuring point, 1.7m from the ground. Point L and M are surface temperature of radiant bed, which are arranged at two equal points of the bed diagonal respectively. The test instruments used for each test parameter are shown in Table 1. The above parameters are automatically collected and recorded by using the Agilent 34970A, intervals remain 10s.

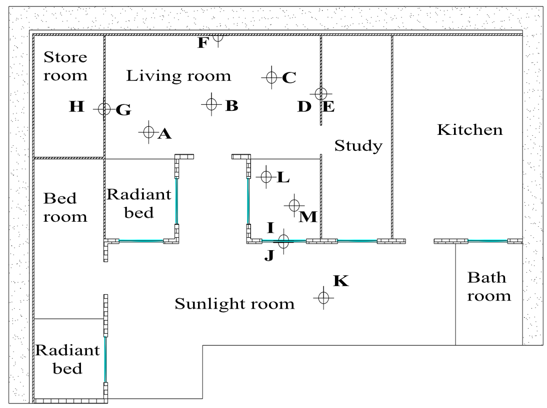

Fig. 3 Testing point map of experimental object

Table 1 Testing parameters and instruments

Number	Parameters	Equipment	Specifications	Output signal
1	Ambient wind speed	FC-2A3	Range：0～30 m/s Accuracy：±3%	Voltage signal：0~5 V
2	Indoor wind speed	YGC-RMFS Hot Film Wind Velocity Sensor	Range：0～5 m/s Accuracy：±0.2% FS	Current signal：4~20 mA
3	Solar radiation intensity	TBQ-2-B Total radiometer	Range：0～2000 W/m^2 Sensitivity：8.963 μV/Wm^{-2}	Voltage signal：0~2.5 V
4	Indoor air temperature	Four-wire Pt-100 Temperature sensor	Range：-50～100 ℃ Accuracy：1/3B级	
5	Indoor humidity	STH-TW1-RHT1OVP2S0 Temperature and humidity transmitter	Range：0～100% RH，Accuracy：±3% RH	Voltage signal：0~5 V
6	Ambient humidity	CWS11-08-A1-G Temperature and humidity transmitter	Range：-40~100 ℃ Accuracy：±5% RH	Voltage signal：0~5 V
7	Flow	LWGY-32A Turbine flowmeter	Range：0.4~8 m^3/h Accuracy：0.5%	Voltage signal：1~5 V
8	SO_2		Range：0-100 mg/m^3	

			Accuracy：0.1 mg/m^3
9	CO	Fixed on-line multi-function four-in-one detector	Range：0-10 mg/m^3 Accuracy：0.01mg/m^3
10	VOC		Range：0-10 mg/m^3 Accuracy：0.1 mg/m^3
11	CO_2		Range：0-2000mg/m^3 Accuracy：±5%
12	PM10 PM2.5	Intelligent On-line Dust Concentration Detector	Range：0.001-10 mg/m^3 Accuracy：0.01mg/m^2

2.3 Date analysis

The average radiant temperature MRT is an important parameter about the indoor thermal environment and it is one of the parameters when considering the indoor heating[16]. The operative temperature t_{op} refers to the temperature that felt by the human. In most practical cases, the operative temperature t_{op} is calculated based on the air temperature and the average radiant temperature.

The average radiation temperature MRT is calculated as :

$$MRT = \sum A_n T_n \Big/ \sum A_n \qquad (1)$$

Where A_n is the inner surface area of each enclosure structure, m^2； T_n is the inner surface temperature of each enclosure structure, ℃.

According to the national standard “Civil Building Indoor Thermal and Humidity Environmental Evaluation Standard”(GB/T 50785-2012)[15], when the air flow rate is less than 0.2 m/s, the operative temperature t_{op} can be approximately equal to the average value of the average radiant temperature MRT and indoor air temperature T_a. A is taken as 0.5.

The operative temperature t_{op} can be calculated as :

$$t_{op} = At_a + (1-A)MRT \qquad (2)$$

Where t_{op} is operative temperature, ℃; t_a is indoor air temperature, ℃; A is coefficient, ℃.

The energy collected by passive sunspace conducted the indoor room through the south wall which is divided into two parts, one is 130 mm red brick with area of 27 m^2, and the other is glass window with total area of 9 m^2. The heating capacity of solar passive system was calculated as :

$$Q_i = \sum (T_{si} - T_{so}) A_i K_i t \qquad (3)$$

Where Qi is the heat conduction through the enclosure, J; T_{si} is the inner wall temperature, ℃; T_{so} is the outer wall temperature, ℃; A_i is the area of the enclosure, m^2; K_i is the heat transfer coefficient of the enclosure, W/(m^2 · K); t is the time, s.

$$K_i = \frac{\lambda_i}{\delta_i} \qquad (4)$$

Where λ_i is the thermal conductivity of the envelope material, W/(m^2 · K); δ_i is the thickness of the envelope material, m.

The heating capacity of solar active system was calculated as :

$$Q = \sum c_p m \left(T_{\text{in}} - T_{\text{out}}\right) t \qquad (5)$$

Where C_P is the specific heat capacity of water, taking 4200 J/(kg C); m is the circulating water flow rate for heating, kg/s; T_{in} is the heating inlet temperature, ℃; T_{out} is the heating outlet temperature, ℃.

People’s indoor thermal sensation is affected by six factors: air temperature, long-wave radiation, air humidity, airflow conditions, and the body’s clothing and activity. Through human experiments, the researchers proposed a variety of evaluation indicators that can describe the effects of environmental parameters on human thermal sensation. Among them, the PMV(Predicted Mean Vote) index, proposed by Prof. Fanger, has became an internationally recognized thermal sensory prediction model under steady-state thermal environment. The PMV indicator represents the feeling of a majority of people in the same environment. However, due to the existence of individual differences, PMV index can’t represent all the people’s feeling. Fanger has also proposed an index PPD(Predicted Percent Dissatisfied) which establishes a quantitative prediction of the percentage of thermally dissatisfied people who feel too cool or too warm[5].

PMV-PPD combines air temperature, relative air velocity, air relative humidity, mean radiant temperature, clothing insulation and human body metabolic rate. It is the most comprehensive thermal environment evaluation index. According to the

"Evaluation Standard for Indoor Thermal and Humid Environment of Civil Buildings" (GB/T 50785-2012), the evaluation level of thermal and humid environment should meet the requirements of Table 2.

Table 2 Overall evaluation index

Level	Overall evaluation index	
Level Ⅰ	PPD≤10%	0.5≤PMV≤0.5
Level Ⅱ	10%＜PPD≤25%	0.5≤|PMV|≤1
Level Ⅲ	PPD＞25%	|PMV|＞1

Calculate the PMV using Equations (1) to (4):

$$PMV = (0.303e^{-0.036M} + 0.028) \times \{(M-W) - 3.05\times10^{-3}\times[5733 - 6.99(M-W) - p_a] - 0.42[(M-W) - 58.15] - 1.7\times10^{-5}M(5867 - p_a) - 0.0014M(34 - t_a) - 3.96\times10^{-8} f_{cl} \times[(t_{cl}+273)^4 - (\bar{t_r}+273)^4] - f_{cl}h_c(t_{cl}-t_a)\} \quad (6)$$

$$t_{cl} = 35.7 - 0.028(M-W) - I_{cl}\{3.96\times10^{-8} f_{cl} [(t_{cl}+273)^4 - (\bar{t_r}+273)^4] + f_{cl}h_c(t_{cl}-t_a)\} \quad (7)$$

$$h_c = \begin{cases} 2.38|t_{cl}-t_a|^{0.25} & 2.38|t_{cl}-t_a|^{0.25} > 12.1\sqrt{v_{ar}} \\ 212.1\sqrt{v_{ar}} & 2.38|t_{cl}-t_a|^{0.25} < 12.1\sqrt{v_{ar}} \end{cases} \quad (8)$$

$$f_{cl} = \begin{cases} 1.00 + 1.290 I_{cl} & I_{cl} \leqslant 0.078\ m^2\cdot K/W \\ 1.05 + 0.645 I_{cl} & I_{cl} > 0.078\ m^2\cdot K/W \end{cases} \quad (9)$$

With the PMV value determined, calculate the PPD using Equation (10),

$$PPD = 100 - 95e^{[-(0.03353PMV^4 + 0.2179PMV^2)]} \quad (10)$$

Where M is the metabolic rate, W/m^2; W is the effective mechanical power, W/m^2; I_{cl} is the clothing insulation, m^2· K/W; f_{cl} is the clothing surface area factor; t_a is the air temperature, ℃; t_r is the mean radiant temperature, ℃; v_{ar} is the relative air velocity, m/s; p_a is the water vapour partial pressure, P; h_c is the convective heat transfer coefficient, W/(m^2· K); t_{cl} is the clothing surface temperature, ℃.

3. RESULTS AND DISCUSSION

3.1 Solar radiation intensity

In the 177 days of the experiment, the solar radiation in Gannan was very well. As shown in Figure 4, The days' number that the total solar radiation is more than 20 MJ/m^2 was 84 days, accounting for 19.2%. The days' number that the total solar radiation ranges from 15 to 20 MJ/m^2 was 34 days, accounting for 19.2%.The combined ratio of two reaches 66.7%, indicating that the region was mostly sunny during the entire heating season. The days' number that solar radiation was less than 10 MJ/m^2 is 26 days, accounting for 14.7%, indicating that only a small number of days were cloudy.

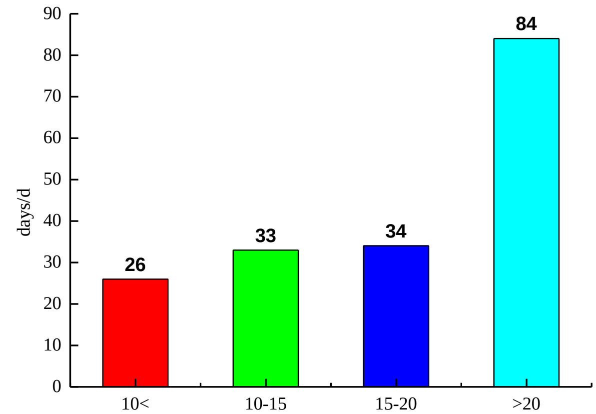

(a) Statistics of days of solar radiation

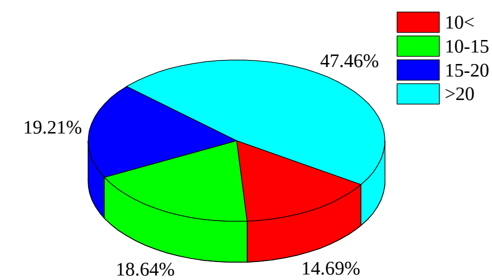

(b) The proportion of days in the range of solar radiation

Fig. 4 Solar radiation quantity of the whole heating season

3.2 The analysis of the active solar heating

The energy collected by the active solar heating system dissipate to the room through the heating circulating pump. As the outdoor heating pipeline is short enough and the insulation of the pipeline is well, the heat loss of the outdoor heating pipeline is neglected. Temperature and flow rate of inlet and outlet water for ground heating are shown in Fig. 5. According to formula (5), the active solar heating system transfers 270.8 MJ of heat to indoor per day, equivalent to 9.24 kg standard coal (the calorific value of standard coal is 29.31 MJ/kg[17]).

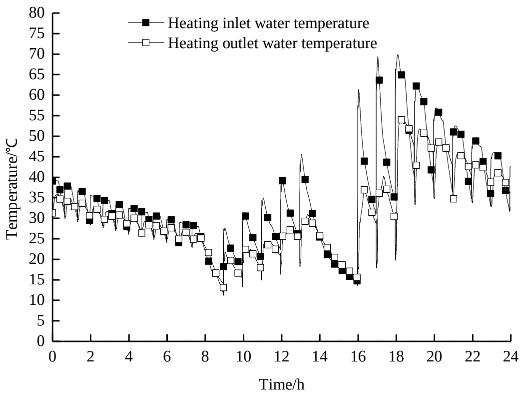

(a)Heating inlet and outlet water temperature

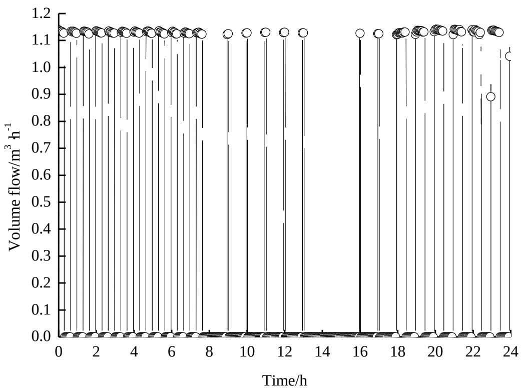

(b) Volume flow rate of heating water

Fig. 5 Temperature and flow rate of inlet and outlet water for ground heating

3.3 The analysis of the passive solar heating

The energy collected by the passive solar heating system mainly through sunspace. The solar radiation intensity in sunshine room is shown in figure 6. Taken the effective area of the sunspace as 47 m^2, the solar radiation entering in the sunspace is 515.12 MJ by calculation. The energy collected by passive sunspace conducted the indoor room through the south wall which is divided into two parts, one is 130 mm red brick with area of 27 m^2, and the other is glass window with total area of 9 m^2. Fig. 6 is the temperature of the inner and outer wall of the south wall. According to formula (3), the solar passive sunshine room can provide 19.6 MJ heat to the indoor through brick wall and 94.1 MJ heat to the indoor through window glass, which is equivalent to 3.9 kg of standard coal.

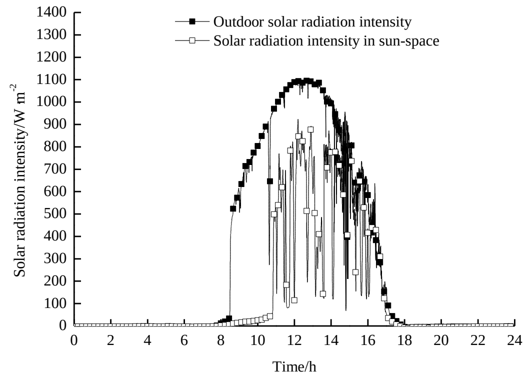

Fig. 6 Solar Radiation Intensity in Sunspace and Outdoor

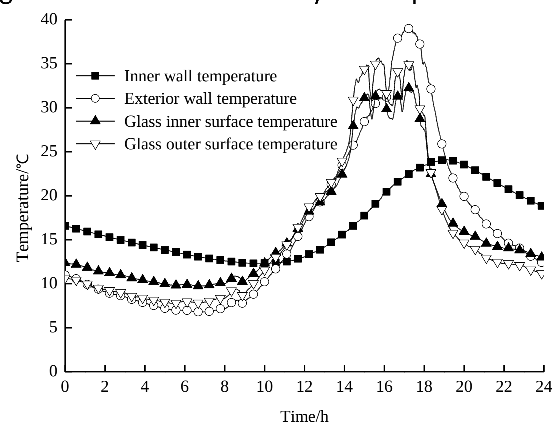

Fig. 7 Temperature of the inner and outer wall of the south wall

3.4 Indoor air temperature

In order to compare the indoor heating effect of the experimental building and the comparative building and the uniformity of the temperature distribution in the heating room, we tested the indoor air temperature of the vertical direction at 0.1, 0.6, 1.1 and 1.7 m respectively according to "the evaluation standard of the indoor heat and humidity environment of civil buildings" (GB/T 50785-2012). Test data for typical days March 5th and 6th are shown in Figure 7 Within two days, the minimum outdoor air temperature was -5.6 ℃ and -10.9 ℃, and the average outdoor air temperature was 0.4 ℃ and -3 ℃, respectively. The temperature difference between day and night was relatively large, 16 ℃ and 18 ℃, respectively. The temperature in the vertical direction of the test building is higher than 14 ℃, which meets the requirements of "Energy-saving Design Standard for Rural Residential Buildings" (GBT50824-2013), and the temperature decreases from bottom to top. The vertical temperature stratification is not obvious. The temperature difference between the adjacent heights is less than 1 ℃, and the maximum temperature difference between the ankle and the head is only about 2 ℃. Contrast with the comparative building, the temperature fluctuates greatly, the amplitude reaches 16 ℃, the night temperature is very low, and the temperature distribution in the vertical direction is uneven. The temperature difference between 1.1m and 1.7m is 5℃. In summary, it can be concluded that the heating effect of the test building has obvious advantages and the indoor temperature distribution is more uniform.

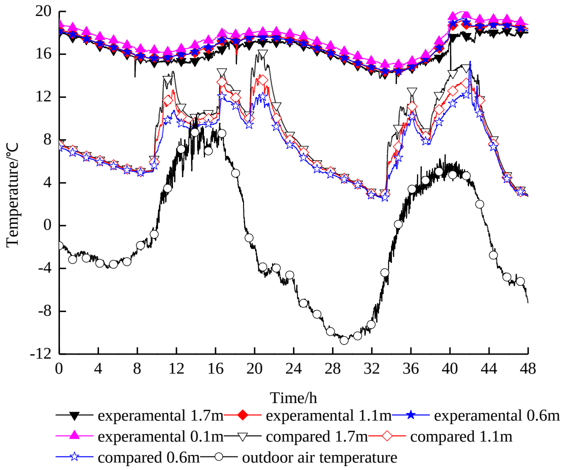

Fig. 8 Vertical temperature distribution in experimental and compared building

3.5 The average radiant temperature and the operative temperature

As shown in Figure 9, it can be seen that the indoor air temperature t_a, the average radiant temperature MRT and the operative temperature t_{op} had the same trend. The average radiant temperature MRT was 13.8~22 ℃ within two days, and the operative temperature top is was 14.5~21 ℃, especially the night when you fall asleep, the two temperatures were 18~20 ℃, the whole room is in very comfortable now.

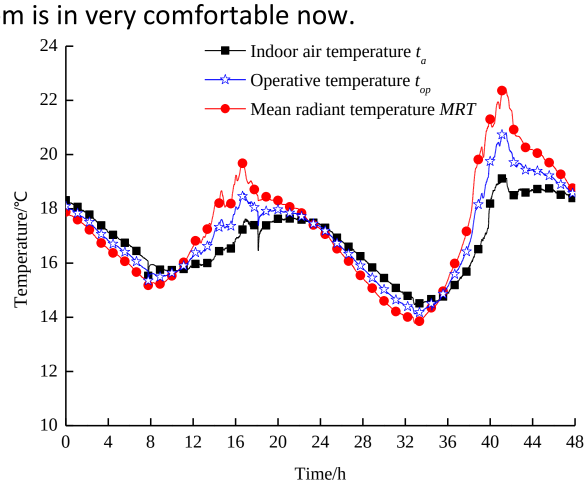

Fig. 9 Mean radiant temperature MRT and operative temperature top of the experimental building

3.6 Indoor relative humidity and wind speed

Indoor relative humidity and wind speed are important indicators describing the indoor thermal environment. When the indoor humidity is high, people will be listless and depressed; when the humidity is low, the skin will be dry, leading to the rapid reproduction of influenza viruses, causing epidemic diseases, and also making people's respiratory system resistance decline, inducing and aggravating respiratory diseases. When the indoor wind speed is too high, people will feel the obvious wind feeling, affecting people's thermal comfort. As shown in Fig. 10, the indoor maximum relative humidity is 55% and the minimum relative humidity is 47% in the experimental building on November 22. The indoor wind speed is close to 0, and there is no wind sense in the experimental building. The indoor maximum relative humidity is 42% and the minimum relative humidity is 32% in the compared building, and the indoor wind speed is higher than that in the experimental building.

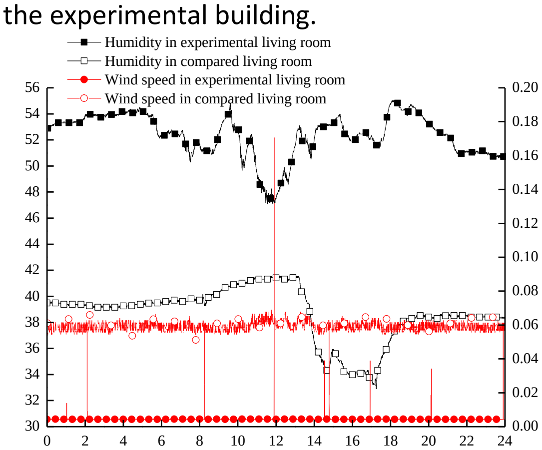

Fig. 10 Relative humidity and wind speed in experimental and compared Building living rooms

3.7 The temperature of water heating Kang

The operation mode of the solar Kang is the same as that of the ground water heating. The heating mode starts at 18:00, the circulating pump working half per an hour, and stops half an hour until 8:00 on the next day. The heating mode ends and the anti-freezing mode is opened. The anti-freezing mode starts and stops once per an hour, working 3 minutes and stopping for 57 minutes. Fig. 10 is the temperature distribution of 9 measuring points on the Kang surface on November 22, 2018 and The temperature trend of 9 measuring points is the same. In the anti-freezing mode, the Kang surface temperature decreases to the lowest value. When the heating mode is opened, the Kang surface temperature rises rapidly to the highest temperature. With the decrease of the water tank temperature, the Kang surface temperature also decreases gradually. There are bedding on the measuring points 1, 4 and 7, so the temperature is obviously higher than that of other measuring points. In the sleep stage (20:00-24:00), the highest temperature is stable at 30-36 C. According to the literature [18], the comfort temperature of human body in the sleep environment is between 29-34 ℃. Therefore, the water heating Kang can well guarantee the thermal comfort of human sleep.

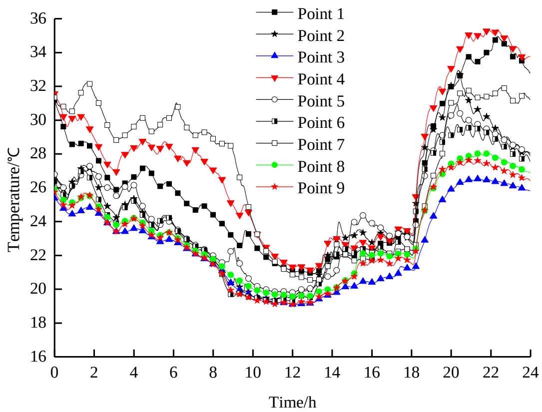

Fig. 11 Surface Temperature of Water Heating Kang

3.8 Indoor air quality

The indoor concentration of SO_2, VOC, CO, CO, CO_2, PM10 and PM2.5 were continuously tested and analyzed, indoor air quality of experimental building and compared building are shown in Fig.11(a) and Fig.11(b) respectively.

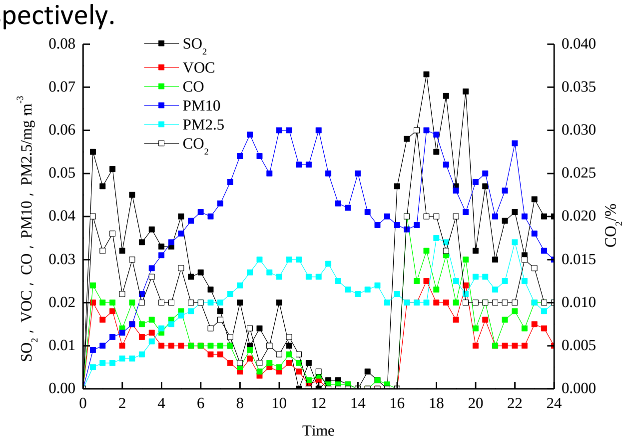

(a) The experimental building

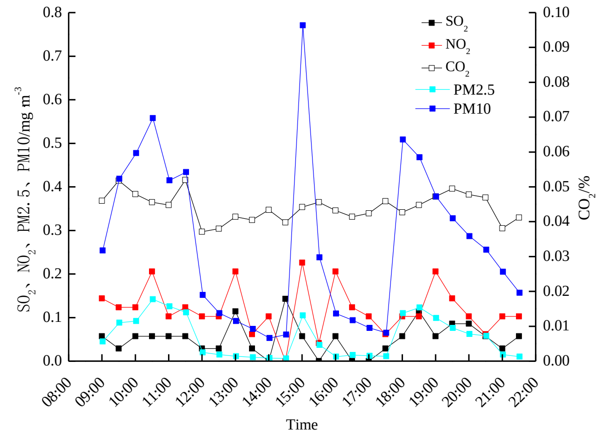

(b) The compared building

Fig. 12 Indoor air quality

In the experimental building, the maximum 1-hour mean values of SO_2 and CO were 0.07 and 0.02 mg/m^3, respectively. The daily average values of CO_2, PM10 and PM2.5 are 0.01, 0.04 and 0.02 mg/m^3, respectively, and the 8-hour average of VOC is 0.01 mg/m^3. These values are far less than the standard values of each index which met the national standard (GBT18883-2002) "Indoor Air Quality Standard". In the compared building, the highest concentration of SO_2 was 0.08 mg/m^3, the highest concentration of NO_2 was 0.16 mg/m^3, the daily average concentration of CO_2 was 0.04%, and the daily average concentration of PM10 and PM2.5 was 0.2 mg/m^3 and 0.05 mg/m^3, in which the concentrations of SO_2, NO_2, CO_2 and PM10 were lower than the standard values, but they were all larger than the experimental building, and PM10 was significantly higher than the standard value. The experimental building has better indoor air quality than compared building.

The comprehensive index evaluation method of indoor air quality is selected to evaluate the air quality in the living room of the experimental building. The method takes the pollutant index, the highest index, the arithmetic average index and the comprehensive index into account, which can reflect the pollution degree of indoor air comprehensively.

The calculation method of composite index I is as follows:

$$I = \sqrt{(\max\left|\frac{C_1}{S_1}, \frac{C_2}{S_2}, \ldots, \frac{C_n}{S_n}\right|)(\frac{1}{n}\sum\frac{C_i}{S_i})} \quad (11)$$

where C_i is actual concentration of pollutants, mg/m^3; S_i is Standard value of pollutants, mg/m^3.

Referring to Table 3, the indoor air quality index calculated by formula (11) can be used to evaluate the indoor air quality.

Table 3 Air quality grade determination

Composite index	Index level	Index category
≤0.49	Ⅰ	Clean
0.50～0.99	Ⅱ	Unpolluted
1.00～1.49	Ⅲ	Light pollution
1.50～1.99	Ⅳ	Moderate pollution
≥2.00	Ⅴ	Heavy pollution

According to the calculation, the comprehensive index of indoor air quality on November 13th is 0.04, and the air quality index is level I, which showed that the indoor is clean. According to the statistics, the indoor air quality of the experimental building met the level I throughout the whole heating season, which showed that the active and passive solar heating buildings have good indoor air quality.

3.9 Indoor thermal comfort

According to the living habits of local residents and referring to the standard, the farmers' metabolic rate M of indoor activity in winter is 70 W/m^2, and the effective mechanical power W could be neglected. The basic dress of the residents are briefs, vest, sweater, jacket, wool pants, outer pants, thick socks and cotton slippers, the average clothing insulation I_{cl} is 1.12 col (0.17 m^2·K/W). The convective heat transfer coefficient h_c and the clothing surface temperature t_{cl} be solved by iteration using C++. Then the metabolic rate M, the clothing insulation I_{cl}, air temperature t_a, mean radiant temperature t_r, the relative air velocity v_{ar} and water vapor partial pressure pa can be taken into the PMV-PPD calculation formula. The calculated statistical results are shown in Figure 12.

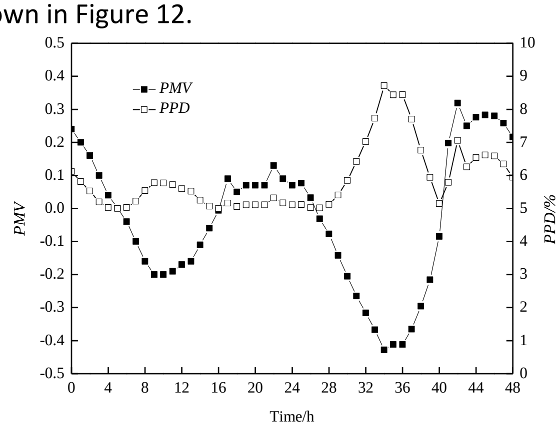

Fig. 13 PMV-PPD indicators March 5th and 6th

4. CONCLUSION

1) Solar energy in Gannan Tibetan Autonomous Prefecture is abundant and the winter sunshine period in this area is long. In the 177 days of the experiment, The days' number that the total solar radiation is more than 15 MJ/m^2 was 118 days, accounting for 66.7%.

2) Compared with the comparative building, the indoor thermal environment of the experimental building is more comfortable. The temperature in the vertical direction of the experimental building is higher than 14 ℃, and the temperature stratification in the vertical direction is not obvious. In contrast, the temperature distribution in the vertical direction of the comparative building is uneven, the maximum temperature difference between 1.1m and 1.7m is 5 ℃. According to the Fanger's PMV-PPD evaluation system, the thermal environment of experimental building is I level (PPD≤10% and -0.5≤PMV≤0.5), the human body feels very comfortable.

3) The indoor air quality of solar active and passive heating buildings was better than that of the traditional heating buildings. The 1-hour average of SO_2 and CO, 8-hour average of VOC, daily average of CO_2, PM10 and PM2.5 in solar active and passive heating buildings all met the requirements of National Standard for Indoor Air Quality (GBT18883-2002). The indoor pollutant concentration of traditional heating buildings was higher than that of solar active and passive heating buildings. The concentration of SO_2, NO_2, CO_2 and PMl0 was lower than the standard value, and PM10 was obviously beyond the standard in case of traditional heating buildings.

ACKNOWLEDGEMENT

This work was supported by National Key Research and Development Program Project (2018YFB0905104), National Natural Science Foundation Project (51676094), Organization Department of Gansu Provincial Party Committee of the Communist Party of China "Longyuan Youth Innovation Talents Support" Project (Innovation Team, Gan Group Tongzi [2014] 93), Gansu University Collaborative Innovation Technology Team Project, Gansu Province International Science and Technology Cooperation Project Project (1604WKCA009), Lanzhou Talent Innovation and Entrepreneurship Project (2017-RC-34), Gansu Natural Science Foundation

(1508RJZA051) and Lanzhou University of Technology Hongliu First-class Discipline Fund.

REFERENCE

[1] Stazi F, Mastrucci A , Perna C D. The behaviour of solar walls in residential buildings with different insulation levels: An experimental and numerical study[J]. Energy and Buildings, 2012, 47(2):217-229.

[2] Ajib S, Jaber S. Optimum design of Trombe wall system in mediterranean region[J]. Solar Energy, 2011, 85(9):1891-1898.

[3] Wei S, Jie J, Luo C, et al. Performance of PV-Trombe wall in winter correlated with south facade design[J]. Applied Energy, 2011, 88(1):224-231.

[4] Rabani M, Kalantar V, Dehghan A A, et al. Experimental study of the heating performance of a Trombe wall with a new design[J]. Solar Energy, 2015, 118(10):359-374.

[5] Sánchez-Ostiz, Ana, Monge-Barrio A, Domingo-Irigoyen S, et al. Design and experimental study of an industrialized sunspace with solar heat storage[J]. Energy and Buildings, 2014, 80(8):231-246.

[6] Oliveti G, Arcuri N, Simone M D, et al. Solar heat gains and operative temperature in attached sunspaces[J]. Renewable Energy, 2012, 39(1):241-249.

[7] Y. Yang. Heat transfer process and energy efficiency evaluation for attached sunapace in dwelling in south of Liaoning [D]. Dalian: Dalian University of Technology, 2015(in Chinese).

[8] D.S. Zhao, J. Ji, H.C. Yu, et al. Numerical and experimental study of a combined solar Chinese Kang and solar air heating system based on Qinghai demonstration building[J]. Energy & Buildings, 2017, 143.

[9] M. Nemś, J. Kasperski, A. Nemś, et al. Validation of a new concept of a solar air heating system with a long-term granite storage bed for a single-family house[J]. Applied Energy, 2018, 215: 384-395.

[10] A. Carotenuto, R.D. Figaj, L. Vanoli, et al, A novel solar-geothermal district heating, cooling and domestic hot water system: Dynamic simulation and energy-economic analysis[J]. Energy, 2017, 141.

[11] I. Sobhy, A. Brakez, B. Benhamou. Energy performance and economic study of a solar floor heating system for a Hammam[J]. Energy and Buildings, 2017, 141: 247-261.

[12] M. Ali, S.A. Khan, N.A. Sheikh, et al. Performance Analysis of a Low Capacity Solar Tower Water Heating System in Climate of Pakistan[J]. Energy & Buildings, 2017: 84–99.

[13] Shan M, Yu T, Yang X. Assessment of an integrated active solar and air-source heat pump water heating system operated within a passive house in a cold climate zone[J]. Renewable Energy, 2016, 87:1059-1066.

[14] Badescu V. Case study for active solar space heating and domestic hot water preparation in a passive house[J]. Journal of Renewable & Sustainable Energy, 2011, 3(2):3-11.

[15] Ministry of Housing and Urban-Rural Construction of the People's Republic of China. Evaluation Criteria for Indoor Thermal and Wet Environment of Civil Buildings: GB/T 50785-2012[S] Beijing: Chinese People's Construction Industry Publishing House, 2012.

[16] LI Jin. Study on Thermal Comfort in Radiant Heating Room[D]. Harbin: Harbin Institute of Technology, 2001(in Chinese).

[17] F. Gui. Boiler Principle (2nd Edition) [M]. Beijing: China Electric Power Press, 2014.

[18] Lin Z, Deng S. A study on the thermal comfort in sleeping environments in the subtropics-Measuring the total insulation values for the bedding systems commonly used in the subtropics[J]. Building & Environment, 2008, 43(5):905-916.

